



Natural variation in Tiller Number 1 affects its interaction with TIF1 to regulate tillering in rice

Quan Zhang^{1,†} , Jianyin Xie^{1,†}, Xiaoyang Zhu¹, Xiaoqian Ma¹, Tao Yang¹, Najeeb Ullah Khan¹, Shuyang Zhang¹, Miaosong Liu¹, Lin Li¹, Yuntao Liang², Yinghua Pan², Danting Li² , Jinjie Li¹ , Zichao Li^{1,3} , Hongliang Zhang^{1,3,4,*}  and Zhanying Zhang^{1,*} 

¹MOE Key Laboratory of Crop Heterosis and Utilization/Beijing Key Laboratory of Crop Genetic Improvement, College of Agronomy and Biotechnology, China Agricultural University, Beijing, China

²Guangxi Key Laboratory of Rice Genetics and Breeding, Rice Research Institute of Guangxi Academy of Agricultural Sciences, Nanning, Guangxi, China

³Sanya Institute of China Agricultural University, Sanya, China

⁴Sanya Nanfan Research Institute of Hainan University, Sanya, China

Received 26 November 2021;

revised 15 December 2022;

accepted 23 January 2023.

*Correspondence (Tel +86-10-62734018;

fax +86-10-62731414; email

zhangzhanying@cau.edu.cn (Z.Z.); Tel +86-

10-62734018; fax +86-10-62731414; email

zhangl@cau.edu.cn (H.Z.)

†These authors contributed equally to this work.

Keywords: rice, tiller number, BAH domain, GWAS, geographical distribution.

Summary

Tiller number per plant—a cardinal component of ideal plant architecture—affects grain yield potential. Thus, alleles positively affecting tillering must be mined to promote genetic improvement. Here, we report a Tiller Number 1 (TN1) protein harbouring a bromo-adjacent homology domain and RNA recognition motifs, identified through genome-wide association study of tiller numbers. Natural variation in TN1 affects its interaction with TIF1 (TN1 interaction factor 1) to affect *DWARF14* expression and negatively regulate tiller number in rice. Further analysis of variations in *TN1* among *indica* genotypes according to geographical distribution revealed that low-tillering varieties with *TN1*-hap^L are concentrated in Southeast Asia and East Asia, whereas high-tillering varieties with *TN1*-hap^H are concentrated in South Asia. Taken together, these results indicate that *TN1* is a tillering regulatory factor whose alleles present apparent preferential utilization across geographical regions. Our findings advance the molecular understanding of tiller development.

Introduction

Rice (*Oryza sativa* L.) is a global staple food. Thus, rice grain yield must be increased to ensure overall food security. Rice yield dramatically increased following 'Green Revolution' in the 1960s, during which semi-dwarfing and heterosis played significant roles (Wang *et al.*, 2017). Ideal plant architecture and high nitrogen-use efficiency (NUE) are the current strategies aimed at improving rice yield (Duan *et al.*, 2019; Sun *et al.*, 2014; Wang and Li, 2006). In rice, tillering is relevant to both ideal plant architecture and high NUE (Liu *et al.*, 2021; Wu *et al.*, 2020). Therefore, exploring the mechanisms of tiller development is important in breeding for ideal plant architecture and high NUE.

The currently cloned genes controlling tiller development in rice primarily regulate the initiation or outgrowth of axillary buds. In particular, *MONOCULM1* (*MOC1*), *MONOCULM3/TILLERS ABSENT1/STERILE* and *REDUCED TILLING 1* (*MOC3/TAB1/SRT1*), *LAX PANICLE1* (*LAX1*), and *LAX PANICLE2/ GRAIN NUMBER PER-PANICLE4* (*LAX2/GNP4*) induce tiller initiation and regulate tiller number (Li *et al.*, 2003; Lu *et al.*, 2015a; Mjomba *et al.*, 2016; Oikawa and Kyozuka, 2009; Tabuchi *et al.*, 2011; Tanaka *et al.*, 2015; Zhang *et al.*, 2011a). Other genes, specifically those involved in the strigolactone (SL) pathway, such as *DWARF3* (*D3*), *DWARF10* (*D10*), *DWARF14/HIGH TILLERING DWARF 2* (*D14/HTD2*), and *DWARF53* (*D53*), regulate tillering by affecting the growth of axillary buds (Arite *et al.*, 2007, 2009; Gao *et al.*, 2009; Ishikawa *et al.*, 2005; Jiang *et al.*, 2013; Liu *et al.*, 2009; Zhou *et al.*, 2013). *D3*, *D53*, and *D14* interact with each other under treatment with GR24

(an SL) leading to ubiquitination of *D53* by *D14* and the SCF^{D3} complex. Loss-of-function mutants *d3* and *d14* and functional-gain mutant *d53* showed markedly increased tiller numbers (Jiang *et al.*, 2013; Zhou *et al.*, 2013). *IDEAL PLANT ARCHITECTURE 1/SOUAMOSA PROMOTER BINDING PROTEIN-LIKE 14* (*IPA1/OsSPL14*) promotes panicle branching and contributes to ideal plant architecture (Jiao *et al.*, 2010; Miura *et al.*, 2010). *D53* interacts with *IPA1* to repress its transcriptional activation, and *IPA1* binds the promoter of *D53* in feedback regulation under SL-mediated signal transduction (Song *et al.*, 2017). Rice *TEOSINTE BRANCHED 1* (*OstB1*) is a negative regulator suppressing axillary bud outgrowth (Minakuchi *et al.*, 2010; Takeda *et al.*, 2003). Furthermore, *OsMADS57* negatively regulates *D14* expression, although its inhibitory activity is weakened upon interaction with *OstB1* (Guo *et al.*, 2013). *IPA1* and *CIRCADIAN CLOCK ASSOCIATED 1* (*OsCCA1*) are the key transcription factors binding the promoter of *OstB1* to restrain tillering, and *OsCCA1* acts upstream of *D14* and *IPA1* to regulate axillary bud outgrowth (Lu *et al.*, 2013; Wang *et al.*, 2020). In addition, *NITROGEN-MEDIATED TILLER GROWTH RESPONSE 5* (*NGR5*) interacts with Polycomb Repressive Complex 2 (*PRC2*), influencing the H3K27me3 modification level of *D14* and *IPA1* to regulate their expression levels (Wu *et al.*, 2020). Overall, there has been extensive research on the regulation of tiller buds.

Typically, bromo-adjacent homology (BAH) domain-containing proteins are attached to chromatin-associated proteins and play important roles in transcriptional regulation and protein–protein interactions (Callebaut *et al.*, 1999; Chambers *et al.*, 2013).

Arabidopsis BAH domain proteins EARLY BOLTING IN SHORT DAY (EBS) and SHORT LIFE (SHL) suppress the transcription of flowering genes (Li *et al.*, 2018; Yang *et al.*, 2018). The BAH domain recognizes the histone marks H3 lysine 9 di-methylation (H3K9me₂), H4 lysine 20 di-methylation (H4K20me₂), H3 lysine 27 tri-methylation (H3K27me₃), and unmodified H3K4 (Du *et al.*, 2012; Kuo *et al.*, 2012; Li *et al.*, 2016, 2018; Yang *et al.*, 2018; Zhang *et al.*, 2020). Majority of the RNA-binding proteins (RBPs) harbour RNA recognition motifs (RRMs) and are primarily involved in post-transcriptional regulation, such as mRNA splicing, 3'-end processing, and mRNA stability and decay (Goodarzi *et al.*, 2014; Hogan *et al.*, 2008; Kenan *et al.*, 1991; Roundtree *et al.*, 2017). OsRRM and OsRRMh-containing RRM play important roles in plant architecture and cell development in rice endosperm (Chen *et al.*, 2007; Liu and Cai, 2013). *Arabidopsis* ANTI-SILENCING 1/INCREASE IN BONSAI METHYLATION 2 (ASI1/IBM2), which contains both a BAH domain and RRM, interacts with ASI1-IMMUNOPRECIPITATED PROTEIN 1 (AIPP1) and ENHANCED DOWNY MILDEW 2 (EDM2) to form the AAE complex to facilitate 3'-distal polyadenylation further, and to stabilize full-length transcripts. The loss of function of ASI1 alters the expression of heterochromatin-containing genes with a high level of DNA or histone methylation in the gene body region (Duan *et al.*, 2017; Saze *et al.*, 2013; Wang *et al.*, 2013). Taken together, these reports indicate that proteins containing BAH domains and RRM play pivotal roles in developmental processes. A recent study showed that OsASI1 (the orthologue of *Arabidopsis* ASI1 in rice) regulates a nuclear XRN family exonuclease gene, *OsXRNL*, which further affects the processing of miRNA precursors (You *et al.*, 2021). However, the functions of proteins containing BAH domains and RRM in the regulation of tiller number remain unknown.

As outlined above, many genes involved in tiller development, including *D3*, *D14*, *D53*, and *OsTB1*, have been identified through mutant studies. However, due to their unfavourable phenotypes, such mutants have little value in crop improvement. Therefore, favourable alleles/haplotypes affecting tillering must be mined from natural populations. It was recently found that tiller-regulating genes usually showed high expression in the root at 24:00. Based on this expression pattern and a genome-wide association study (GWAS), a *small auxin-UP RNA* gene, *OsSAUR27*, was identified in natural populations and has been proven to affect tiller number and plant architecture (Ma *et al.*, 2020).

To this end, in this study, we performed GWAS on tiller number and identified a tillering regulator, Tiller Number 1 (TN1)/OsASI1, containing a BAH domain and an RRM. Its functional variation site (+2163G > A) is located in the first exon. We further showed that TN1 interacts with TIF1 (TN1 interaction factor 1) to positively regulate *D14* expression and modulate axillary bud outgrowth, ultimately affecting tiller development. We observed that *TN1* has not been under selection during rice domestication, although various haplotypes have been established in different regions. Our results enrich the gene pool for the genetic improvement of tillering in cultivated rice.

Results

Candidate gene analysis of locus *qTN2*

In a panel of 295 cultivated rice accessions, tiller number per plant ranged from 3.7 to 19.0 (Dataset S1). Association analysis using a

mixed linear model (MLM) with the top three principal components (PCs) as the fixed effects (Figure S1) revealed 13 quantitative trait loci (QTLs) associated with tiller number, which were named *qTN1–qTN13* (Dataset S2). As *qTN2* showed the strongest signal in GWAS (Figure 1a and Figure S2a), candidate genes in a 122 kb interval of *qTN2* were screened and 12 genes were identified (Figure 1b, Dataset S3). Expression data from RiceXPro website (Sato *et al.*, 2011) indicated that five of these genes produced no transcripts at any growth stage. Thus, we analysed haplotypes of the remaining seven genes and found no significant differences in the expression levels of these genes among the different haplotype varieties (Figure 1d, Figures S2d and S3). Of these, only *LOC_Os01g42460* and *LOC_Os01g42490* possess significant non-synonymous SNPs in the functional encoding regions. The expression analysis showed that *LOC_Os01g42460* in roots at 24:00 during vegetative growth was significantly higher than that of *LOC_Os01g42490* (Figure S2b). Additionally, the expression level of *LOC_Os01g42460* at the base of tiller buds at 45 days after transplanting was significantly higher than that of *LOC_Os01g42490* (Figure S2c). These results prompted us to focus further on *LOC_Os01g42460*, which we named *TN1*.

Using six significant SNP variants above the suggestive significance threshold of GWAS in the promoter and protein coding regions, we identified four *TN1* haplotypes (hap1, hap2, hap3, and hap4) in the *indica* subpopulation and one haplotype (hap2) in the *japonica* subpopulation (Figure 1c,d). In the *indica* subpopulation, tiller numbers in hap1, hap2, and hap3 accessions were similar, being significantly higher than in hap4. This implied that the SNP (+2163G > A) in the coding region causing a mutation at the 83rd amino acid (arginine/glutamine) of the BAH domain may be the functional variation. Meanwhile, a previous study showed that a mis-sense substitution in BAH_{EBS} decreases the binding activity of *EBS*, thereby affecting flowering in *Arabidopsis* (Li *et al.*, 2018; Pineiro *et al.*, 2003). Then, we tested the promoter activities of three haplotypes (hap1, hap2, and hap4) in rice protoplasts but noted no significant differences (Figure S2e,f). Meanwhile, there were no obvious differences in the expression level of *TN1* in *indica* accessions containing hap1, hap2 (high tiller), and hap4 (low tiller) (Figure S2d). Collectively, these results suggest that the non-synonymous SNP variant (+2163G > A) of *LOC_Os01g42460* is vital for the tiller development and is the most probable candidate gene.

TN1 negatively regulates tiller formation in rice

TN1 encodes a protein with 502 amino acids (aa) and contains a BAH domain (amino acid 28–145) and an RRM (amino acid 340–416). To identify whether *TN1/LOC_Os01g42460* regulates tiller number, we knocked out the BAH domain or RRM in separate lines. Mutant *tn1-1* carried a 6 bp deletion in the first exon, resulting in a 3 amino acid change in the BAH domain compared with the wild-type Nipponbare (NIP). Mutants *tn1-2* and *tn1-3* carried a 4 bp deletion and a 1 bp insertion, respectively, in the sixth exon of *TN1*; both mutations were located in the RRM and caused frameshifts (Figure 2a and Figure S4a,b). Mutant *tn1-4* carried a thymine (T) insertion in the BAH domain, causing premature termination (Figure S4b). Tiller number in *tn1-1* and *tn1-4* increased by 29.8% and 31.7% compared with that in NIP, while the number in *tn1-2* and *tn1-3* was not significantly different from that in NIP (Figure 2b–e and Figure S4c). Thus, the BAH domain might play an important role in tillering regulation. Further, we introduced the coding sequence (CDS) of *TN1* driven by the CaMV35S promoter into NIP to generate constitutive *TN1*-

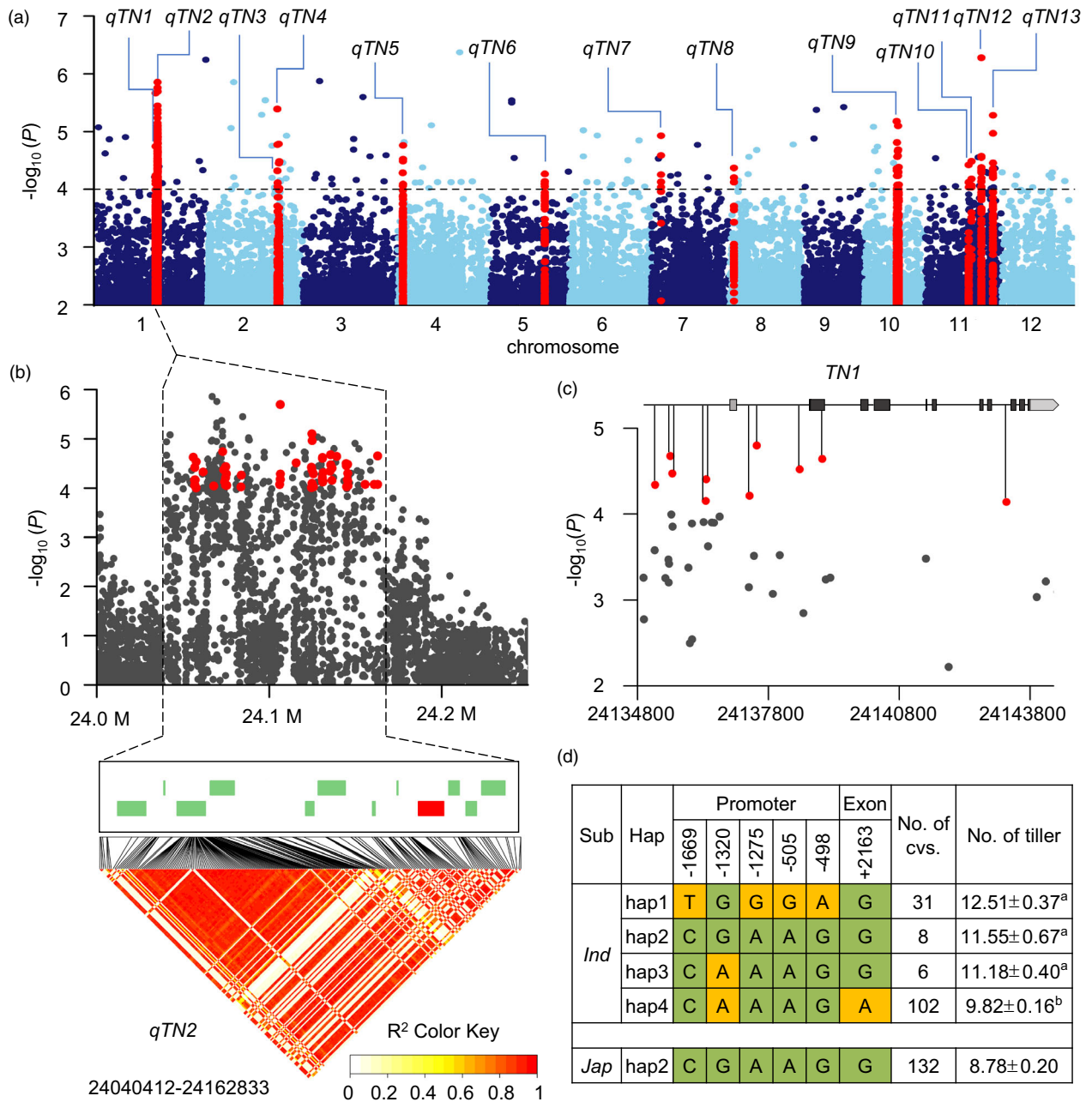
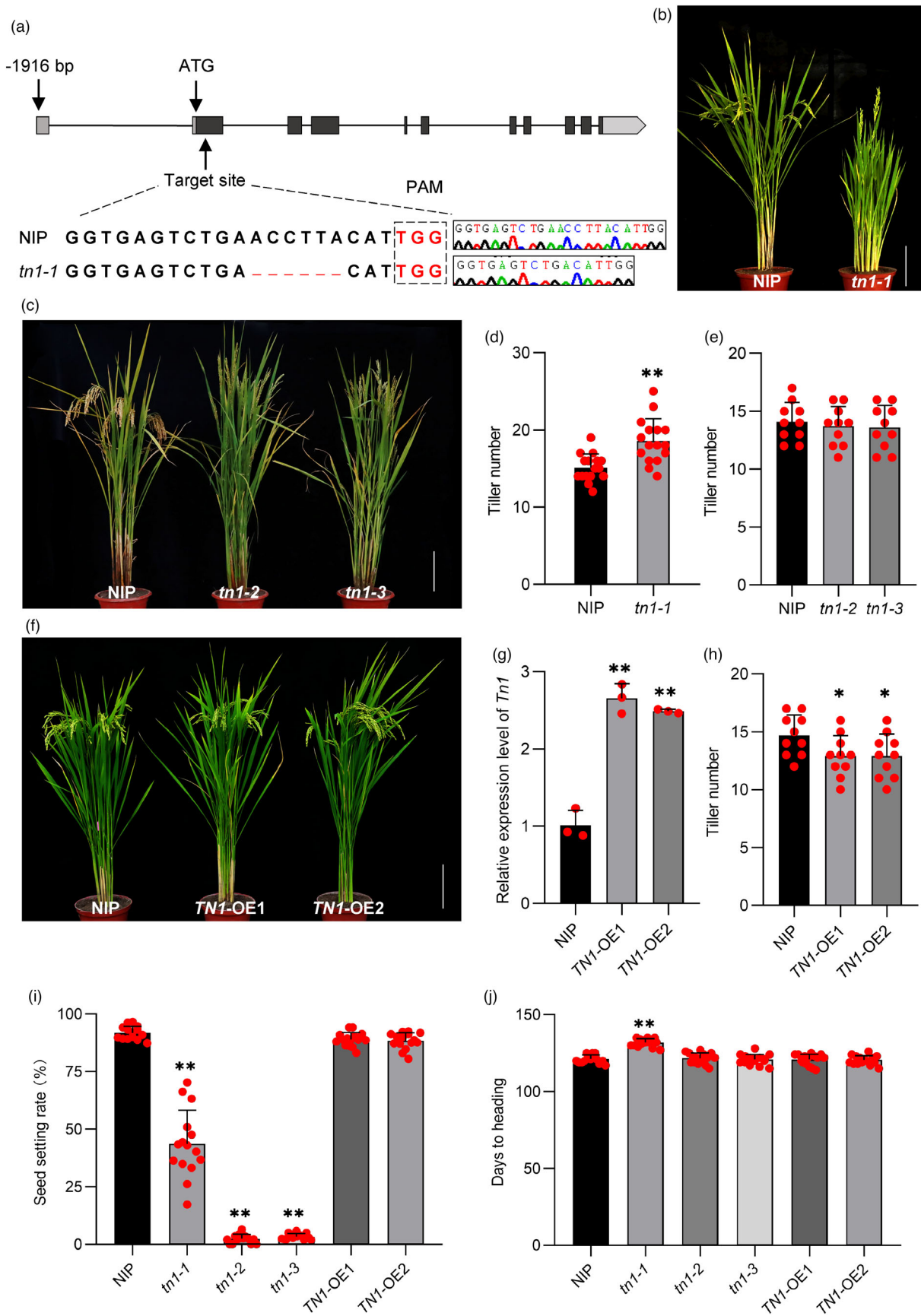


Figure 1 GWAS of tiller number to identify *TN1*. (a) Manhattan plot of GWAS results. Red dots represent QTLs. (b) Regional Manhattan plot of *qTN2* and pairwise LD analysis. Significant SNPs ($-\log_{10}(P) \geq 4$) are presented as red dots. Green and red boxes indicate annotated genes, triangles denote QTLs, and dots represent SNPs. (c) *TN1*-based association mapping. Red dots indicate SNPs ($-\log_{10}(P) \geq 4$) in the 2000 bp promoter and 7467 bp genomic sequence. (d) Haplotypes (hap) of *TN1* among 279 accessions; major and minor alleles are indicated in yellow and green respectively. Data are presented as mean \pm SE. Different letters indicate significant differences at $P < 0.05$ according to two-tailed Student's *t*-test.

overexpression lines. Tiller number in *TN1*-OE1 and *TN1*-OE2 was significantly reduced compared with that in NIP (Figure 2f–h). Moreover, the initiation of tillering buds was not affected in either

tn1-1 or *TN1*-OE (Figure S5). Taken together, these results indicate that *TN1* negatively controls tillering growth to affect tiller number.

Figure 2 Phenotypic characterization of *TN1*-transgenic plants. (a) Sequences of CRISPR-knockout lines. (b) Phenotypes of NIP and *tn1-1* lines at the reproductive stage. Scale bar = 20 cm. (c) Phenotypes of NIP and *tn1-2* and *tn1-3* lines at the reproductive stage. Scale bar = 20 cm. (d) Tiller number per plant of NIP and *tn1-1* lines. (e) Tiller number per plant of NIP and *tn1-2* and *tn1-3* lines. (f) Phenotype of NIP and *TN1*-OE lines at the reproductive stage. Scale bar = 20 cm. (g) Expression level of *TN1* in NIP versus *TN1*-OE lines. Data are presented as mean \pm SD. ($n = 3$ biologically independent samples). (h) Tiller number per plant of NIP and *TN1*-OE lines. (i) Seed setting rate of NIP, *tn1-1*, *tn1-2*, *tn1-3*, and *TN1*-OE lines. (j) Heading date of NIP, *tn1-1*, *tn1-2*, *tn1-3*, and *TN1*-OE lines. In (d–j), *P*-values were determined using two-tailed Student's *t*-tests. $**P < 0.01$. Data are presented as mean \pm SD ($n = 15$).



Expression patterns of *TN1*

To determine the subcellular localization of TN1, we transformed the 35S:*TN1-GFP* vector into rice protoplasts and tobacco leaves. The results showed that TN1 is a nuclear protein (Figure 3a and Figure S6). Analysis of dynamic *TN1* expression in different tissues (Figure S7a,b) revealed high expression in tiller buds at 30 and 60 days after transplanting (DT_30 and DT_60 respectively). In addition, we generated *ProTN1:GUS* transgenic plants and detected strong GUS activity in tiller buds (Figure 3b,e). These results are consistent with the function of *TN1* in regulating tiller growth.

Tn1 recognizes the H3K27me3 mark and interacts with TIF1

We blasted the TN1 protein and noted that it is highly homologous to *Arabidopsis* ASI1/IBM2 (Figure 4a). Given that both these proteins harbour a BAH domain and this domain can recognize a series of histone marks, we performed a histone pull-down assay and found that TN1 could bind the H3K27me3 mark (Figure 4b). H3K27me3 is a histone mark that suppress gene expression; thus, TN1 may recognize the H3K27me3 mark of downstream genes to regulate their expression.

To clarify the molecular mechanism of *TN1*, we cloned the homologous proteins of AIPP1 and EDM2 in rice. LOC_Os07g15270 and LOC_Os08g24946 shared the highest homology with AIPP1 and EDM2 (Figure S8a) and were named TN1 interaction factor 1 (TIF1) and OsEDM2 respectively. Yeast two-hybrid (Y2H) assays showed that TN1, TIF1, and OsEDM2 did not exhibit transactivation activity (Figure S9a). TN1^{hap4} showed a stronger interaction with TIF1 than TN1^{hap1} *in vitro* (Figure 4c). Likewise, these differences in interaction intensity were observed in luciferase complementation image (LCI) assays (Figure 4d). In addition, subcellular localization assay revealed that TIF1 is a nuclear protein (Figure S8b). Therefore, bimolecular fluorescence complementation (BiFC) assay was performed in rice protoplasts and tobacco leaves, together with co-immunoprecipitation (Co-IP) assays, which further confirmed the interaction between TN1 and TIF1 *in vivo* (Figure 4e, f and

Figure S8c). However, both TN1 and TIF1 did not interact with OsEDM2 in yeast, and yeast three-hybrid (Y3H) assays showed no complex formation between TN1, TIF1, and OsEDM2 (Figure S9a–c).

TIF1 is a negative regulator of tiller number in rice

TIF1 showed a similar expression pattern to *TN1*, with high expression in tiller buds at 30 days after transplanting (Figure 5a). To investigate the function of *TIF1*, we knocked out *TIF1* with CRISPR–Cas9 using two target sites located in the first exon (Figure 5b) and obtained two homozygous mutant lines, namely *tif1-1* and *tif1-2*. The former harboured a 73 bp deletion between the two target sites, and the latter carried a 2 bp deletion at the first site and a 1 bp insertion at the second site, with both causing frameshifts that resulted in early translation termination (Figure 5b). Similar to that in *tn1-1*, tiller number was significantly increased in *tif1-1* and *tif1-2* compared with that in NIP (Figure 5c,d). These results indicate that *TIF1* and *TN1* co-regulate tiller formation in rice.

TN1 and TIF1 affect *D14* expression to regulate tiller development

In *Arabidopsis*, *ASI1* regulates polyadenylation to ensure the transcription of downstream target genes (Saze et al., 2013; Wang et al., 2013). To identify genes downstream of *TN1*, we conducted RNA-Seq analysis and determined differentially expressed genes (DEGs) at the base of axillary buds between NIP and *tn1-1* (Dataset S4). A total of 2938 genes were down-regulated [$\log_2(tn1-1/NIP) \leq -1$, $P < 0.05$] and 2840 genes were up-regulated [$\log_2(tn1-1/NIP) \geq 1$, $P < 0.05$] in *tn1-1* plants (Figure 6a). Gene ontology (GO) analysis revealed that 5778 specific DEGs were enriched in fundamental biological processes (Figure S10a). The Kyoto Encyclopedia of Genes and Genomes (KEGG) pathway analysis showed that many DEGs were enriched in the mRNA surveillance pathway (Figure S10b). These results indicate that *TN1* might also be required for the expression of intragenic heterochromatin-containing genes.

Next, the expression levels of seven cloned genes controlling tiller development, namely *DWARF AND LOW-TILLERING/DLT*

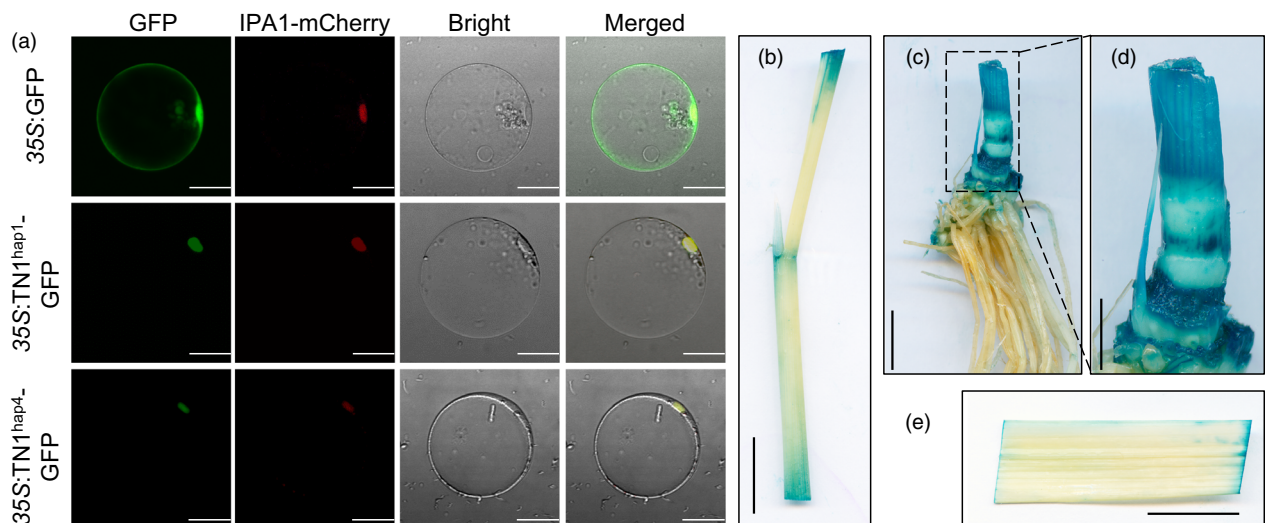


Figure 3 Expression pattern of *TN1*. (a) Subcellular localization of *TN1*-GFP fusion protein in rice protoplasts of different haplotypes. Scale bar = 20 μ m. (b, c, e) GUS staining of tissues (leaf sheath, tiller, and leaf respectively) in *ProTN1:GUS*-transgenic plants at 30 days after transplanting. Scale bar = 2 cm. (d) Enlarged version of dashed box in (c). Scale bar = 1 cm.

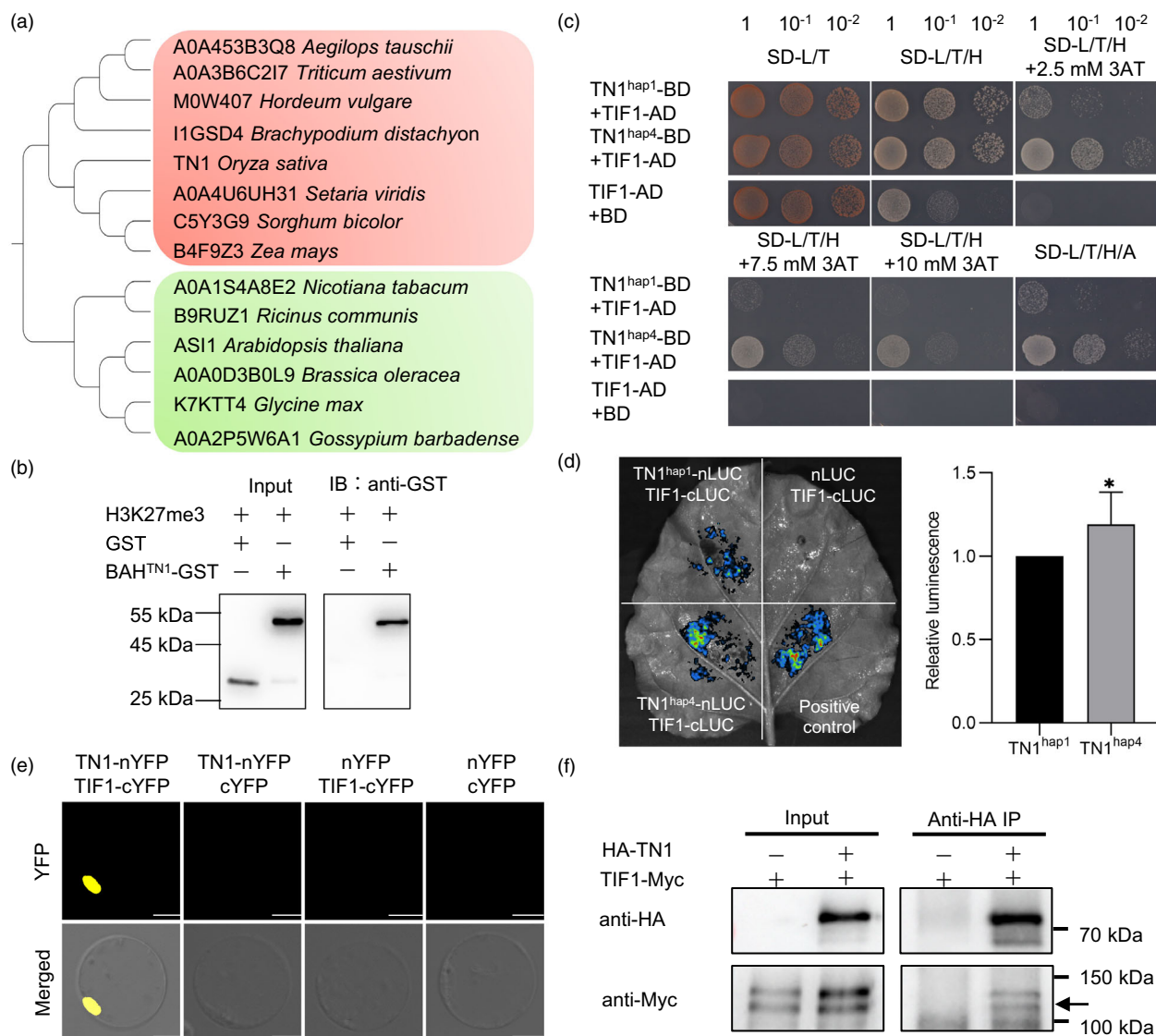


Figure 4 TN1 interacts with TIF1. (a) Phylogenetic analysis of the TN1 protein in 14 species. Monocots and dicots are indicated in orange and green respectively. (b) TN1 recognizes the H3K27me3 peptide in pull-down assay. (c) Yeast two-hybrid assay showing interactions of different genotypes of TN1 with TIF1. (d) Luciferase complementation image (LCI) assay in *Nicotiana Benthamian* leaves. The fluorescence intensity of TN1^{hap1} and TIF1 was set as 1, and the assay was repeated eight times. (e) Bimolecular fluorescence complementation (BiFC) assay in rice protoplasts. Scale bar = 10 μm. (f) TN1 directly interacts with TIF1 in Co-IP assay. Black arrow indicates TIF1-Myc.

(Tong *et al.*, 2009), *OsPIN2* (Chen *et al.*, 2012), *OsPIN5b* (Lu *et al.*, 2015b), *D14*, *D3*, *OstB1*, and *OsCCA1*, were altered in *tn1-1* compared with those in NIP (Figure 6b). The expression patterns of these genes in *tn1-1* were consistent with their functions in promoting tiller formation. Next, we assessed the expression levels of these genes in *tn1-1* and *TN1*-OE lines using qRT-PCR and found that the expression of *OsCCA1*, *D3*, and *D14* was significantly decreased in *tn1-1* but increased in *TN1*-OE1 and *TN1*-OE2 compared with that in NIP (Figure 6c and Figure S11a–d). These results indicate that *TN1* positively regulates the expression of *OsCCA1*, *D3*, and *D14*. *OsCCA1*, *D3*, and *D14* are involved in the same pathway controlling tiller development (Wang *et al.*, 2020). These results prompted us to investigate whether TN1 acts upstream of the *OsCCA1*–*D3*–*D14* module. In addition, we found the expression level of *TIF1* remained unaffected in *tn1-1* or *TN1*-OE (Figure S11e).

Given that *D14* expression is related to the H3K27me3 modification level, we considered that TN1 may recognize the H3K27me3 histone mark of *D14* to affect its expression. We next generated *D14*-overexpression lines in the *tn1-1* background and found that the positive overexpression lines developed less tillers than *tn1-1* (Figure 6d–f). Moreover, the expression levels of *D14*, *D3*, and *OsCCA1* were significantly decreased in the *tif1-1* and *tif1-2* mutants compared with those in NIP (Figure 6c), suggesting that TIF1 also affects the expression of these genes to regulate tiller number. Collectively, these results indicate that TN1 and TIF1 regulate tiller number by affecting *D14* transcription (Figure 6g).

Natural variations in the *TN1* gene

A diverse panel of 2154 cultivated and 221 wild rice accessions (Huang *et al.*, 2012; Wang *et al.*, 2018) was used to investigate variations in *TN1* in various rice germplasms. Based on the SNP

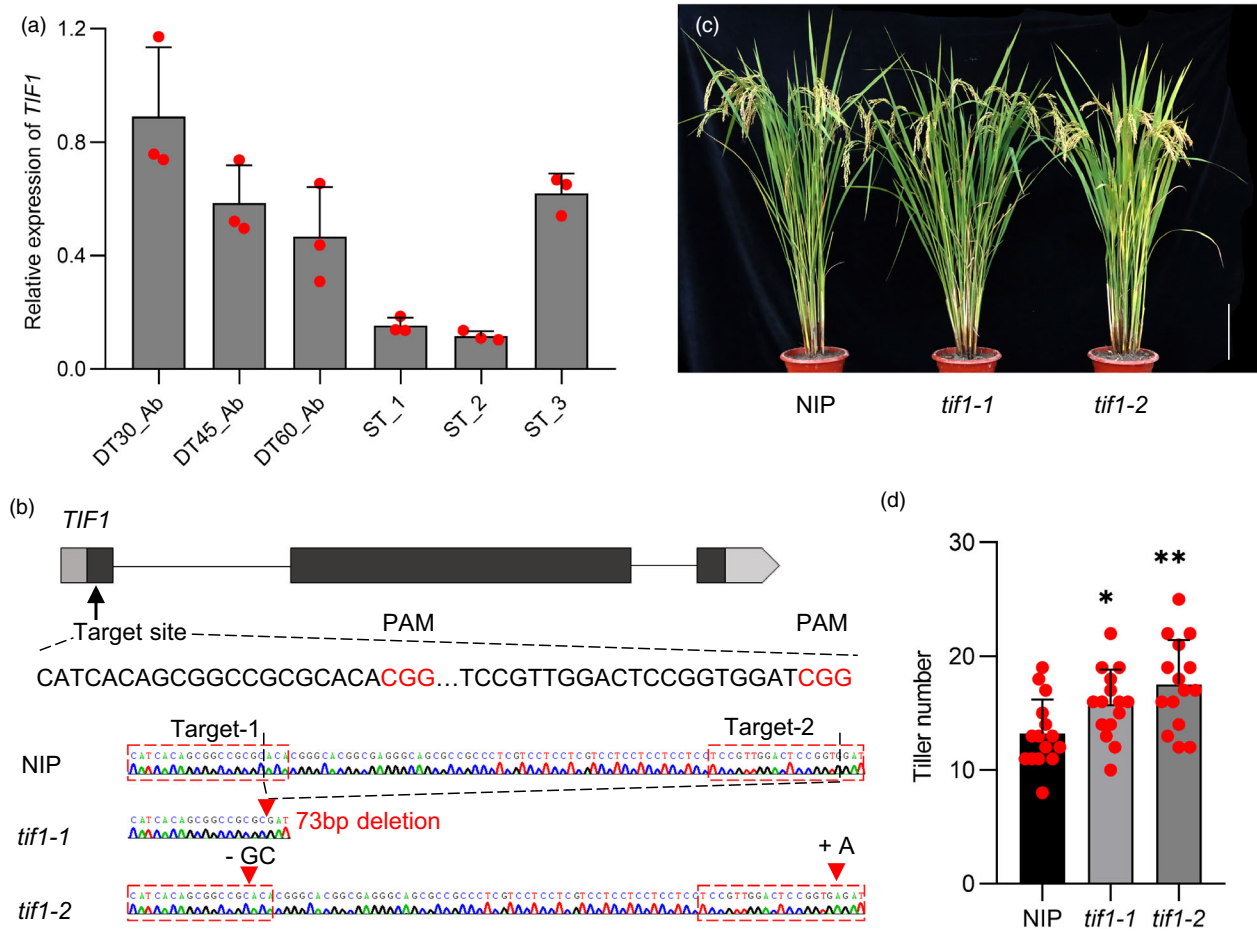


Figure 5 *TIF1* negatively regulates tiller number in rice. (a) Expression levels of *TN1* in tillering tissues. Data are presented as mean \pm SD ($n = 3$ independent biological samples). DT30_Ab, DT45_Ab, DT60_Ab, ST_1, ST_2, and ST_3 represent developmental stages described in Materials and Methods. (b) Mutation targets of *tif1-1* and *tif1-2*. (c) Phenotypes of NIP and *tif1*-CRISPR lines at the reproductive stage. Scale bar = 20 cm. (d) Tiller number per plant of NIP and *tif1*-CRISPR lines. *P*-values were determined using two-tailed Student's *t*-tests. ***P* < 0.01. Data are presented as mean \pm SD ($n = 15$).

variation +2163G > A, the accessions were divided into two haplotypes, namely *TN1*-hap^H (SNP_G) and *TN1*-hap^L (SNP_A). Phylogenetic analysis revealed that *Tn1*-hap^H (SNP_G) and *Tn1*-hap^L (SNP_A) were present in both cultivated and wild rice, indicating that differentiation of *TN1* originated in wild rice. *TN1*-hap^L was present only in the *indica* subgroup, while *TN1*-hap^H was present both in *indica* and *japonica* subgroups (Figure 7a,b). Haplotype network analysis showed *TN1*-hap^L and *TN1*-hap^H were similarly distributed in cultivated and wild rice accessions (Figure S12). We next analysed the nucleotide diversity and Tajima's *D* value of eight subpopulations (*Or-I*, *Or-II*, *Or-III*, *Aus*, *Aro*, *Ind*, *GJ-trp*, and *GJ-trp*) and observed no significant differences in Tajima's *D* value (Table S1), indicating that there has been no selective divergence of *TN1* haplotypes. Investigation of the geographical distribution of *TN1* alleles revealed that *TN1*-hap^L accessions are mainly concentrated in Southeast and East Asia, whereas most *TN1*-hap^H accessions are concentrated in South Asia (Figure 7c). These results indicate apparent preferential utilization of *TN1* alleles across geographical regions. We constructed a near-isogenic line (NIL), NIL-*TN1*^{CH1230}, with *TN1*-hap^H from CH1230 in a 93–11 genetic background (Figure S13). NIL-*TN1*^{CH1230} developed more tillers and showed an earlier

heading date than NIL-*TN1*⁹³⁻¹¹ (Figure 7d), while there were no significant differences in plant height, spikelet number per panicle, and 1000-grain weight. The results indicate that the *TN1*-hap^H allele could be used to promote more tillers. However, the frequency of the *TN1*-hap^L allele was increased in improved varieties (IMPs) compared with that in landraces (LAN), indicating the utilization of *TN1*-hap^L in modern rice varieties (Figure 7f).

We further analysed *TIF1* and found three haplotypes, namely *TIF1*-Hap1, *TIF1*-Hap2, and *TIF1*-Hap3. *TIF1*-Hap1 and *TIF1*-Hap2 were present in both *indica* and *japonica* subgroups, while *TIF1*-Hap3 was present only in the *indica* subgroups (Figure S14). Accessions containing *TIF1*-Hap3 developed less tillers than accessions containing the other two haplotypes. We further conducted a joint haplotype analysis of *TN1* and *TIF1*. A panel of 264 accessions was divided into five haplotypes, H1–H5. H1, carrying *TN1*-hap^H and *TIF1*-Hap1 exhibited the highest tiller number. Therefore, it can be used as an elite haplotype in breeding (Figure 7g). Furthermore, the expression level of *D14* in H1 and H2 varieties was lower than that in H3 and H4 varieties, indicating that the different combinations of *TN1* and *TIF1* in germplasm affect *D14* expression to regulate tiller number (Figure S15).

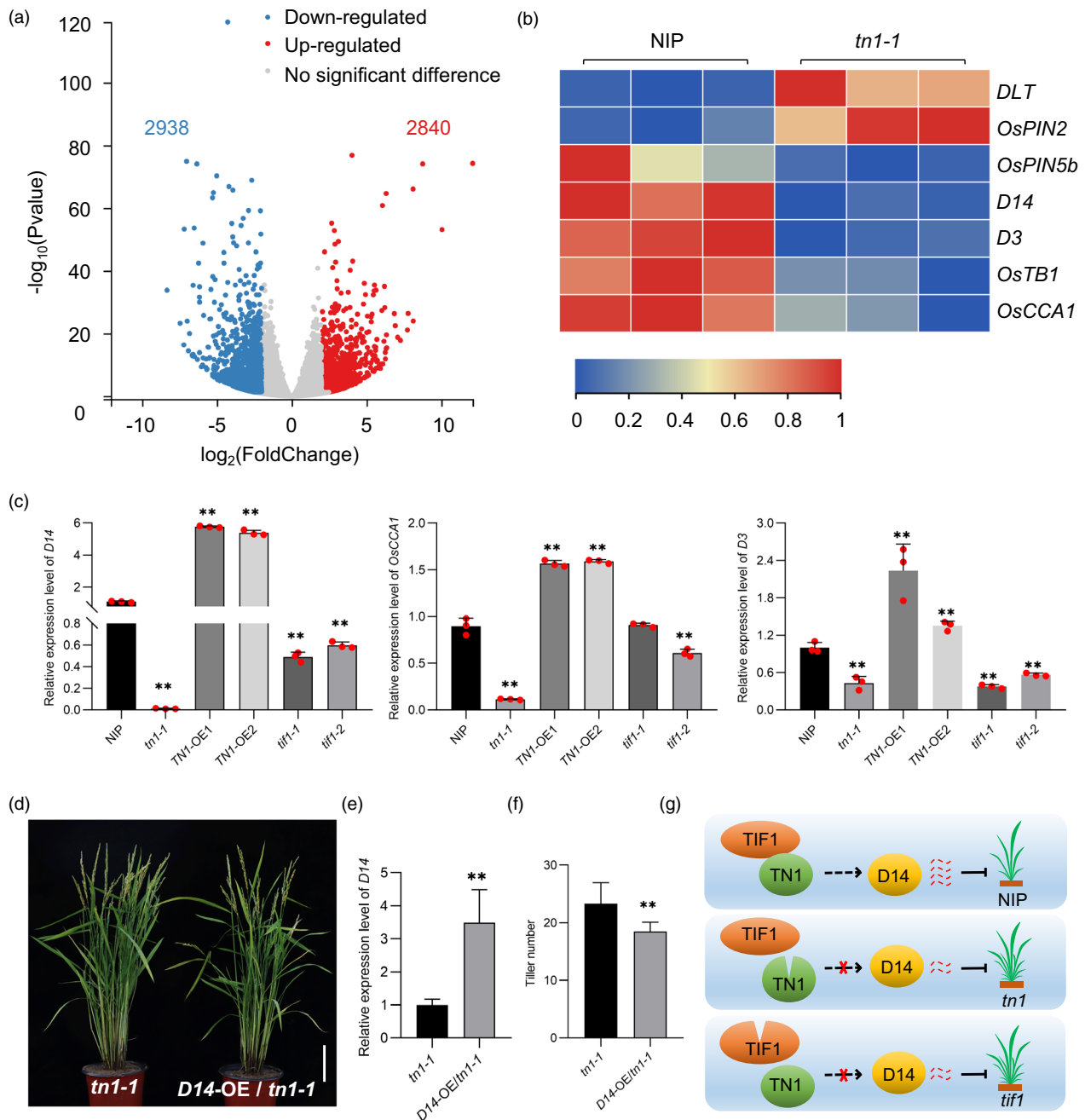


Figure 6 Both TN1 and TIF1 regulate *D14* expression. (a) Volcano map of differentially expressed genes between NIP and *tn1-1*. (b) Heat map showing the expression of tillering-related genes in NIP and *tn1-1*. (c) Relative expression levels of *D14*, *OsCCA1*, and *D3* in NIP, *tn1-1*, *TN1-OE*, and *tif1* lines. (d) Phenotypes of *tn1-1* and *D14-OE/tn1-1* lines at the reproductive stage. Scale bar = 10 cm. (e, f) *D14* expression and tiller number in *tn1-1* and *D14-OE/tn1-1* lines at the reproductive stage. (g) Model of TN1 and TIF1 functioning synergistically to regulate tiller number by affecting *D14* transcripts. Red dotted lines indicate transcript abundance. Dotted circles indicate dysfunctionality. Solid circles indicate full function. Broken circles indicate loss of function. Red crosses indicated inhibition. Data in (c) and (e) are presented as mean \pm SD of three biologically independent samples.

Discussion

TN1 is a homologue of *Arabidopsis* AS11/IBM2, harbouring a BAH domain and an RRM. *OsAS11* has been reported to modulate miRNA and pollen development in rice (You *et al.*, 2021). In this study, *TN1*, a novel allele was identified from rice germplasm participating in tiller development. Based on the phenotypes of transgenic materials (Figure 2b,c and Figure S4c), we further discovered a novel function of the BAH domain and found that

TN1 is involved in multiple pathways. From our results, we proposed a mechanism in which TN1 interacts with TIF1 to affect *D14* expression for regulating tiller number in rice. Furthermore, we noted natural variation in *TN1* (*TN1*-hap^H and *TN1*-hap^L) according to geographical distribution, highlighting its potential use in breeding.

Here, the BAH domain and RRM were separately knocked out using CRISPR-Cas9 to explore their respective functions. Proteins containing the BAH domain, such as EBS, SHL, and AIPP3, have

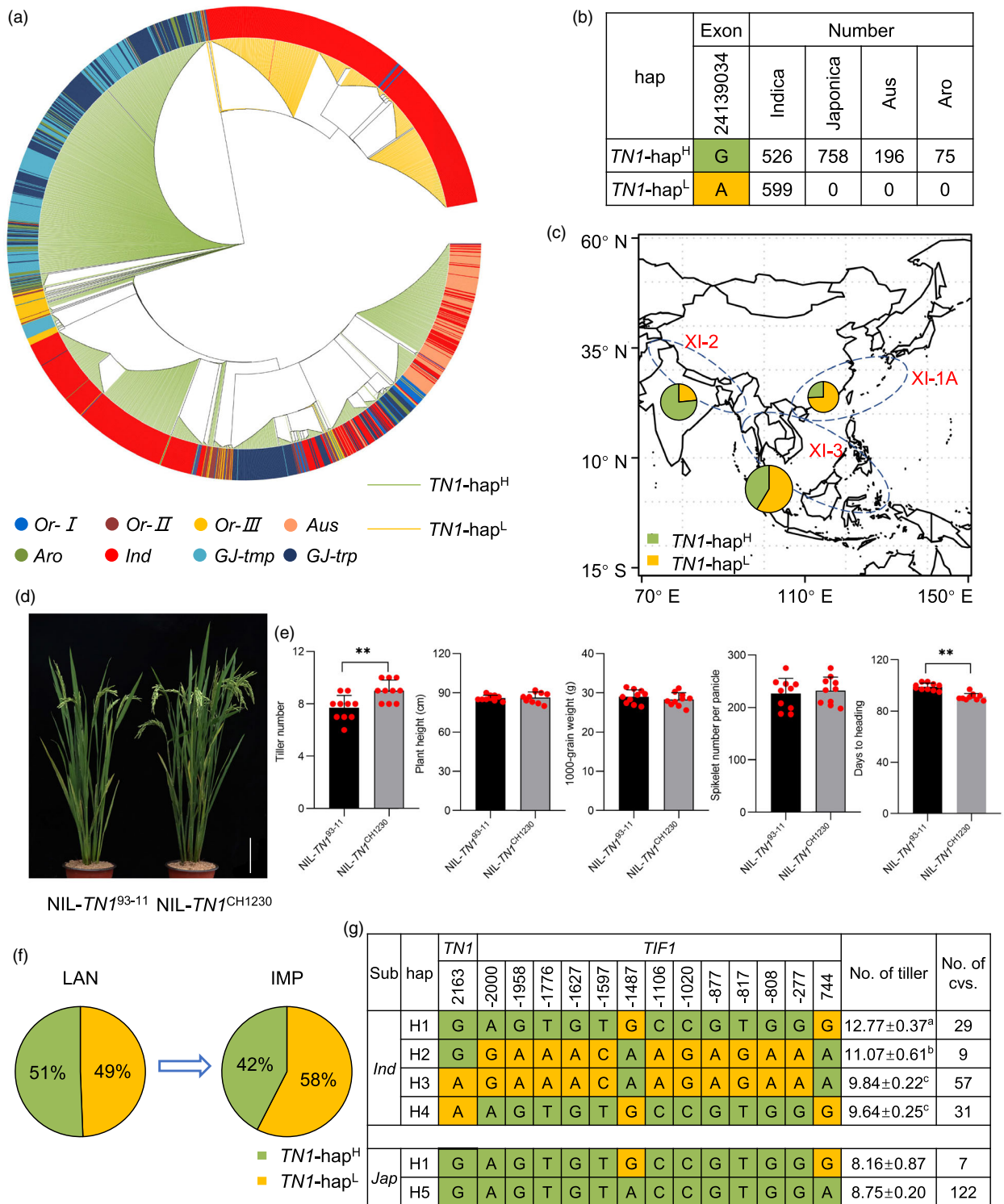


Figure 7 Phylogenetic origins and utilization of *TN1* in breeding. (a) Phylogenetic analysis of *TN1* in a natural rice population. Colour of the outer circle refers to eight ecological groups, including *Or-I*, *Or-II*, *Or-III*, *Ind* (*XI-1A*, *XI-1B*, *XI-2*, and *XI-3*), *temperate japonica* (*GJ-tmp*), *tropical japonica* (*GJ-trp*), *Aus*, and *aromatic* (*Aro*). Inner solid colours indicate the two haplotypes: *TN1-hap^H* and *TN1-hap^L*. (b) Haplotype analysis of the functional SNPs of *TN1*. Colours correspond to the inner branch in (a). (c) Frequencies of *TN1-hap^H* and *TN1-hap^L* in ecotypes *XI-1A*, *XI-2*, and *XI-3*. (d-e) Phenotypes of *NIL-TN1⁹³⁻¹¹* and *NIL-TN1^{CH1230}* at the reproductive stage. (f) Frequency of alleles in improved varieties (IMP) and landraces (LAN). (g) Combined haplotype analysis of *TN1-TIF1* in the *indica* subpopulation.

been shown to regulate flowering time in *Arabidopsis* (Li et al., 2018; Yang et al., 2018; Zhang et al., 2020). In this study, the *tn1-1* line with a 6 bp deletion in the BAH domain developed

more tillers, whereas the *tn1-2* and *tn1-3* lines were similar to WT in terms of tiller number. In *tn1-4*, mutation in the BAH domain resulted in early translation termination, and these lines presented

more tillers than NIP. These results indicate that the BAH domain is involved in tiller development. MEIOSIS ARRESTED AT LEPTOTENE2 (MEL2) is an RRM protein participating in the transition to meiosis at the proper timing. The mutation of *MEL2* causes pollen abortion and decreased seed setting rate (Miyazaki *et al.*, 2015; Nonomura *et al.*, 2011; Zhao *et al.*, 2021). The *tn1-2*, *tn1-3* (Figure 2i), and *tn1-4* (Figure S4c) lines lacking RRM presented a descending fertility phenotype compared with NIP. Although *tn1-1* harboured a complete RRM, its seed setting rate decreased to 47%. In addition, *tn1-1* presented a low seed setting rate, mainly because of delayed heading date (Figure 2j). Rice plants with this phenotype suffer chilling damage during the grain filling stage in Beijing. Meanwhile, *tn1-4* harboured abnormal BAH domain and exhibited a late heading date (Figure S4c), while *tn1-2* and *tn1-3* with intact BAH domains showed normal flowering time (Figure 2j). Therefore, the BAH domain also affects heading date. However, there were no differences between *TN1*-OE and NIP in terms of heading date and seed setting rate (Figure 2i,j).

Previous studies have reported that ASI1 interacts with EDM2 in *Arabidopsis* through an AIPP1 bridge protein, which is involved in post-transcriptional regulation. These proteins form a complex to ensure correct transcription of genes with heterochromatin in their introns (Duan *et al.*, 2017; Saze *et al.*, 2013; Wang *et al.*, 2013). However, in this study, examination of interactions among *TN1*, *TIF1*, and *OsEDM2* showed that only *TN1* and *TIF1* interacted with each other to control tiller number. This result differs from the tripartite interaction reported in *Arabidopsis* (Duan *et al.*, 2017), indicating that the molecular mechanism of *TN1* varies across species or that *TN1* may form a complex with other proteins allied to AIPP1 or EDM2.

The rice loss-of-function mutant *d14* exhibited increased tiller number, whereas *D14*-overexpressing plants were phenotypically similar to the WT plants (Zhao *et al.*, 2014). Tiller number in *tn1-1* was similar to that in *d14*. Overexpression of full-length *D14* in *tn1-1* (*D14*-OE/*tn1-1*) decreased tiller number in *tn1-1*, indicating that *D14* acts downstream of *TN1* (Figure 6g). Furthermore, the expression level of *D14* was lower in the *tif1* mutant (Figure 6c). From these results, we proposed a model in which the functional loss of either *TN1* or *TIF1* decreases the amount of *D14* transcripts to regulate tiller number. In addition, we tested the expression level of *D14* in multiple germplasms and noted that *H1*, *H2*, *H3*, and *H4* with different genotype combinations of *TN1* and *TIF1* showed different *D14* transcript accumulation (Figure S16), as *TN1*^{hap1} and *TN1*^{hap4} formed different interactions with *TIF1* (Figure 4c,d). These results indicate that *TN1* and *TIF1* coordinately regulate *D14* expression to affect tiller number. This model is similar to the mechanism where *OsMADS57* interacts with *TB1* to modulate rice tillering via *D14* expression (Guo *et al.*, 2013). We also tested the expression of *TN1*, *D3*, and *OsCCA1* in *tif1* lines and found that *TN1* and *D3* transcript levels were decreased in both *tif1* lines, while *OsCCA1* transcript level was decreased only in *tif1-2* (Figure 6c, Figure S11f). The results indicate that *TIF1* not only interacts with *TN1* but also affects its expression. However, the mechanism underlying *TIF1*-mediated regulation of *TN1* warrants further research in the future.

ASI1 is involved in polyadenylation to control the position of poly A in *Arabidopsis*. Although we found no alternative 3'-splicing of *D14* in *tn1-1* lines (Dataset S5), a recent study has shown that the interaction of NGR5 with the PRC2 complex alters the H3K27me3 modification level in the *D14* genomic region to regulate its expression (Wu *et al.*, 2020). In a previous study,

variations of the BAH domain were shown to affect binding capability to histone peptides (Li *et al.*, 2018). We also found *TN1* recognizes H3K27me3 (Figure 4f). Meanwhile, two types of *TN1* protein, namely *TN1*^{hap1} and *TN1*^{hap4}, exhibited differential interaction capability with *TIF1* (Figure 4b), suggesting that variations of the BAH domain affect its biological function. Therefore, we speculate that *TIF1* interacts with *TN1*^{hap1} and *TN1*^{hap4} differently, leading to the differential recognition of H3K27me3 by *TN1* to affect *D14* expression for controlling tiller number.

Tillering is a complex phenotype, and different approaches are used to improve tiller utilization. Yield per plant can be increased by increasing the number of effective tillers. However, tiller number decreases with increasing plant density, albeit with little effect on grain yield per unit area (Huang *et al.*, 2016). Evidently, both *TN1*-hap^L and *TN1*-hap^H have been utilized in rice domestication, albeit with different origins. *TN1*-hap^L varieties are mainly present in Southeast Asia and East Asia, whereas most *TN1*-hap^H varieties are present in South Asia. The geographical distribution of the *TN1* allele is similar to that of *OsTCP19* (Liu *et al.*, 2021). Varieties with high- and low-tillering haplotypes are more abundant in nitrogen-poor and nitrogen-rich regions respectively. We also found *TN1* expression was induced by nitrogen (Figure S16). Therefore, *TN1*-hap^H may be responsive to nitrogen fertilization. In recent times, an ideal plant architecture with fewer tillers has been advocated in China and by the International Rice Research Institute in The Philippines (Jiao *et al.*, 2010; Khush, 1995; Virk *et al.*, 2004). The high proportion of improved varieties with *TN1*-hap^L may be attributed to the advocated breeding strategy. *Indica* rice is classified into two major genetic subgroups, *indica I* (*IndI*) and *indica II* (*IndII*), and yield heterosis in superior 3-line hybrid rice cultivars is achieved through crosses between *IndI* and *IndII* accessions, such as the cross between Zhenshan97 (*IndI*) and Minghui63 (*IndII*) (Xie *et al.*, 2015; Lv *et al.*, 2020). In this study, Zhenshan97 presented *TN1*-hap^L, while Minghui63 presented *TN1*-hap^H, indicating that *TN1* may also contribute to heterosis.

Materials and methods

Plant material

A panel of 295 *Oryza sativa* accessions, including 117 accessions from the core collection (Zhang *et al.*, 2011b) and 178 accessions from the International Rice Molecular Breeding Program (Wang *et al.*, 2018; Yu *et al.*, 2003), was planted in the Shangzhuang Experimental Farm of China Agricultural University in Beijing, China (39°9' N, 116°3' E). Five plants in the middle row were randomly selected from each accession to determine tiller statistics. The phenotypes of all materials used for GWAS are listed in Dataset S1. To construct near isogenic lines (NILs) of *TN1*, we developed pairs of molecular markers located in the *TN1* genome region (Dataset S6) and produced a BC₃F₂ NILs using marker selection from the donor variety CH1230 (hap1) to recurrent parent 93-11 (hap4).

Vector construction and genetic transformation

A 20 bp specific sequence from the first exon of the *TN1* CDS was selected and integrated into SK-gRNA to construct the *TN1*-CRISPR vector, as described previously (Wang *et al.*, 2015). A protospacer adjacent motif sequence from the RRM was integrated into pHUE411 to construct the *TN1*-RRM-CRISPR vector (Xing *et al.*, 2014). The *TN1* CDS without the stop codon was integrated

into pSuper1300-GFP to construct the *TN1* overexpression vector. A 2.6 kb promoter fragment upstream of *TN1* was fused to pMDC162 to construct a *ProTN1:GUS* vector. The above constructs were transformed into *Agrobacterium tumefaciens* strain EHA105. The *tn1-1*, *tn1-2*, *tn1-3*, and *tn1-4* transgenic lines were obtained through *Agrobacterium*-mediated infection of NIP (*Oryza sativa* L. subsp. *japonica*) callus. The *D14* CDS without the stop codon was integrated into pMDC32 to construct the *D14-OE* vector, which was transformed into *tn1-1* line to obtain *D14-OE/tn1-1* lines. *D14-OE/tn1-1* lines were planted in Sanya, the other transgenic lines in Beijing during May to October.

GWAS, QTL gene annotation, and haplotype analysis

Sequencing data were derived from the 3000 Rice Genome Project. Association analysis using MLM was performed in TASSEL 5.0. After 1000 permutation analyses, we adopted a threshold of $P = 10^{-4}$ at a genome-wide level. The standard of delimiting QTL followed previously described methods (Huang et al., 2010). A QTL was defined as a region containing least three clustered significant SNPs within a distance of <170 kb between one another. Non-synonymous SNPs were separated from all SNPs identified in the 295 accessions based on information on MSU-RGAP 7.0. Haplotype division was based on significant SNPs (above the suggestive significance threshold of association) concurrently located in the 2 kb promoter and exon of genes.

qRT-PCR

Total RNA was extracted from different plant tissues using TRIzol reagent (Invitrogen, Carlsbad) and treated with RNase-free DNase I. cDNA was generated from 1 µg RNA using M-MLV reverse transcriptase (Takara, Osaka, Japan). qRT-PCR was performed using TB Premix Ex Taq II with ROX Reference Dye II (Takara, #RR820A) on the Applied Biosystems 7500 Fast Real-Time PCR System. Rice *ubiquitin1* was used as the internal control (Dataset S6). Relative gene expression level was analysed using the comparative critical threshold ($\Delta\Delta Ct$) method (Livak and Schmittgen, 2001). RNA for expression pattern analysis was extracted from the base of tiller buds at 30, 45, and 60 days after transplanting (DT_30, DT_45, and DT_60 respectively) and the base of first, second, and third internode at 75 days after transplanting (ST_1, ST_2, and ST_3 respectively).

Subcellular localization

Different haplotypes of *TN1* CDS were cloned and used to generate 35 *S:TN1-hap1*-GFP and 35 *S:TN1-hap4*-GFP vectors for subcellular localization assays. All isolated plasmids were transformed into rice protoplasts using polyethylene glycol-mediated transformation. Fluorescence was examined under a two-photon laser confocal microscope (Zeiss LSM880) after 16 h of growth in the dark.

GUS staining

The solution buffer for GUS staining contained 50 mM Na₂HPO₄, 10 mM Na₂EDTA, 0.5 mM K₃Fe (CN)₆, 0.5 mM K₄Fe (CN)₆, 0.1% Triton X-100, and 1 mg/mL 1,5-bromo-4-chloro-3-indolyl β-D-glucuronic acid. Different tissues of *ProTN1:GUS* transgenic plants were dipped into GUS staining buffer at 37°C for 12 h and then decolorized with 95% alcohol to remove chlorophyll.

BiFC assays

The *TN1* and *TIF1* CDSs were cloned from NIP and integrated into plasmids pUC-SPYNE/pSPYNE-35 S and pUC-SPYCE/pSPYCE-

35 S respectively. *TN1*-nYFP and *TIF1*-cYFP plasmids were co-transformed into rice protoplasts, and mixed *Agrobacterium* suspension containing the *TN1*-nYFP and *TIF1*-cYFP plasmids was injected into *Nicotiana benthamiana* (tobacco) leaves. YFP signals in the rice protoplasts and tobacco leaves was observed after 16 and 48 h under a confocal laser scanning microscope.

Y2H and Y3H assays

Y2H assays were performed according to the manufacturer's recommendations (Clontech). The integrated vectors pGBKT7-TN1 and pGADT7-TIF1 were co-transformed into yeast strain Y2HGold. The yeast cells were plated onto SD-LT (lacking Leu and Trp) and SD-LT/H/A (lacking Leu, Trp, His, and Ade) to assess interactions. Y3H assays were performed as previously described (Zhang et al., 2018). The selective media SD-LT/M (lacking Leu, Trp, and Met) and SD-LT/M/H (lacking Leu, Trp, Met, and His) were used to assess interactions. OD of yeast suspension was set to the same value as that before the test to determine interaction intensity.

LCI assay

The *TN1* and *TIF1* CDSs were fused to the pCAMBIA1300-nLUC and pCAMBIA1300-cLUC vectors respectively. Then, the *TN1*-nLUC and *TIF1*-cLUC vectors were transfected into *Agrobacterium tumefaciens* (strain EHA105) and co-transformed into tobacco leaves. After incubation for 48 h, the leaves were sprayed with 1 mM beetle luciferin solution (Promega, E1605), and LUC signals were observed with a cooled CCD imaging instrument (Vilber, Fusion FX7 EDGE).

Dual-luciferase assay

According to haplotype analysis in the *indica* subpopulation, we cloned 2.6 kb promoter fragments of *TN1* from CH1230 (hap1) and 93–11 (hap4) and inserted them into a *pGreenII0800-LUC* vector to generate *proTN1-hap1-LUC* and *proTN1-hap4-LUC*. All vectors were transformed into rice protoplasts. The activities of firefly luciferase (LUC) and *Renilla* luciferase (REN) were examined using the Dual-Luciferase Reporter Assay System kit (Promega, E1910). LUC/REN results were used to measure the activities of different promoters, and an empty *pGreenII0800-LUC* vector was used as the control. Four replicates were set for the analysis of each vector.

Co-IP assays

Co-IP assays were performed as previously described (Zhang et al., 2017, 2020). HA-TN1 and TIF1-Myc were expressed separately as well as jointly in tobacco leaves. Proteins were extracted from the tobacco leaves and detected with primary anti-Myc (Sigma, M4439) and anti-HA (Sigma, H3663), followed by secondary goat anti-mouse IgG (Light chain specific) (Easybio, BE0105).

RNA-Seq

RNA samples with three biological replicates were collected from the bases of axillary buds in NIP and *tn1-1* lines at 55 days after transplanting. Sample extraction and Illumina sequencing were performed by the Beijing Genome Institute (Wuhan). Clean reads were mapped to the rice genome (MSU-RGAP 7.0) using Bowtie2 (v2.2.5). Gene expression levels were calculated based on RSEM. A volcano map of differentially expressed genes between the wildtype (NIP) and *tn1-1* was plotted using Hiplot (<https://hiplot.com.cn/>). A heat map was plotted using TBtools (<https://github.com/CJ-Chen/TBtools>). All changes in gene expression are presented in Dataset S4.

Nucleotide diversity and selection analysis

A 7.5 kb genomic sequence of *TN1* plus a 2 kb upstream region was used for analysis. Rice groups classified in the 3 K project were examined using DnaSP 5.10.

Evolutionary analysis of TN1 and its genome sequence

Homologous protein sequences of TN1 and TIF1 were downloaded from UniProt (<https://www.uniprot.org/blast/>). A neighbour-joining tree (1000 replications of bootstrap tests) containing 14 species was constructed using MEGA 6.0. The EvolView tool (Zhang *et al.*, 2012) was used to visualize the evolutionary tree.

A panel of 2154 cultivated and 221 wild rice varieties was used to construct a phylogenetic tree of the *TN1* gene sequence according to previously described methods (Li *et al.*, 2021). A minimum spanning tree of haplotypes using the same data was calculated following a previously described method (Guo *et al.*, 2020).

Histone peptide pull-down assay

A part of TN1 CDS (amino acid 1–190) was integrated into pGEX-6P-1 vector, which was transformed into *E. coli* BL21 to purify the TN1-BAH protein; an empty pGEX-6P-1 vector was used as the control. A pull-down assay was performed as previously described (Li *et al.*, 2018; Zhang *et al.*, 2017, 2020). Next, 15 µL of streptavidin beads (NEB, S1421S) and 2 µg of H3K27me3 histone peptide (ANASPEC, AS-64367) were incubated in a binding buffer for 1 h at 4°C. After washing three to five times with a binding buffer to remove free peptides, 2–3 µg of purified TN1-BAH-GST or GST was added to 800 µL of binding buffer with a mixture of beads and H3K27me3 peptides and gently agitated two to three times. Then, 100 µL of the mixture was absorbed as the input sample. The remaining 700 µL of buffer was induced at 4°C for 3 h. The protein–bead mixture was washed five times with a binding buffer before immunoblotting using an anti-GST antibody (Abcam, ab92, 1:2000). Western blots were observed with a cooled CCD imaging instrument (Vilber, Fusion FX7 EDGE).

Primers

Primers used in the study are listed in Dataset S6.

Acknowledgements

We thank Robert A. McIntosh (University of Sydney) for critical reading and suggested revisions for the article. Our confocal observation and western signal detection were performed at the CAB Public Instrument Platform of Chinese Agricultural University and we thank Chen Sun for her help. This work was supported by grants from the National Natural Science Foundation of China (32172030, 31971922, 32272123 and 32072036), the project of the Administrative Bureau of Sanya Yazhou Bay Science and Technology City (SYND-2022-29, B21HJ0508), the Ministry of Science and Technology of the People's Republic of China (2016YFD0100803-2), and the open project of GKLRGB-SKLAB union laboratory, Guangxi Academy of Agricultural Sciences (2018-15-Z06-KF10, 2022-36-Z01-KF03).

Author contributions

Q. Z, Z. Z, and H. Z designed the research. Q. Z and J. X performed data analysis. Q. Z performed most of experiments. X.

Z, Q. M, T. Y, S. Z, M. L, and L. L performed part of the experiments. Y. L, Y. P, D. L, J. L, and Z. L provided technical assistance. Q. Z wrote the article. N.U. Khan assisted with revisions for the article. H. Z, Z. Z, and Z. L conceived and supervised the writing.

Conflict of interest

The authors declare that they have no competing interests.

References

- Arite, T., Iwata, H., Ohshima, K., Maekawa, M., Nakajima, M., Kojima, M., Sakakibara, H. *et al.* (2007) *DWARF10*, an *RMS1/MAX4/DAD1* ortholog, controls lateral bud outgrowth in rice. *Plant J.* **51**, 1019–1029.
- Arite, T., Umehara, M., Ishikawa, S., Hanada, A., Maekawa, M., Yamaguchi, S. and Kyoizuka, J. (2009) *d14*, a strigolactone-insensitive mutant of rice, shows an accelerated outgrowth of tillers. *Plant Cell Physiol.* **50**, 1416–1424.
- Callebaut, I., Courvalin, J.C. and Mornon, J.P. (1999) The BAH (bromo-adjacent homology) domain: a link between DNA methylation, replication and transcriptional regulation. *FEBS Lett.* **446**, 189–193.
- Chambers, A., Pearl, L., Oliver, A. and Downs, J. (2013) The BAH domain of Rsc2 is a histone H3 binding domain. *Nucleic Acids Res.* **41**, 9168–9182.
- Chen, S., Wang, Z. and Cai, X. (2007) *OsRRM*, a *Spem*-like rice gene expressed specifically in the endosperm. *Cell Res.* **17**, 713–721.
- Chen, Y., Fan, X., Song, W., Zhang, Y. and Xu, G. (2012) Over-expression of *OsPIN2* leads to increased tiller numbers, angle and shorter plant height through suppression of *OsLAZY1*. *Plant Biotechnol. J.* **10**, 139–149.
- Du, J., Zhong, X., Bernatavichute, Y.V., Stroud, H., Feng, S., Caro, E., Vashisht, A.A. *et al.* (2012) Dual binding of chromomethylase domains to H3K9me2-containing nucleosomes directs DNA methylation in plants. *Cell* **151**, 167–180.
- Duan, C., Wang, X., Zhang, L., Xiong, X., Zhang, Z., Tang, K., Pan, L. *et al.* (2017) A protein complex regulates RNA processing of intronic heterochromatin-containing genes in *Arabidopsis*. *Proc. Natl. Acad. Sci. U. S. A.* **114**, E7377–E7384.
- Duan, E., Wang, Y., Li, X., Lin, Q., Zhang, T., Wang, Y., Zhou, C. *et al.* (2019) *OsSH1* regulates plant architecture through modulating the transcriptional activity of *IPA1* in rice. *Plant Cell* **31**, 1026–1042.
- Gao, Z., Qian, Q., Liu, X., Yan, M., Feng, Q., Dong, G., Liu, J. *et al.* (2009) *Dwarf 88*, a novel putative esterase gene affecting architecture of rice plant. *Plant Mol. Biol.* **71**, 265–276.
- Goodarzi, H., Zhang, S., Buss, C.G., Fish, L., Tavazoie, S. and Tavazoie, S.F. (2014) Metastasis-suppressor transcript destabilization through TARBP2 binding of mRNA hairpins. *Nature* **513**, 256–260.
- Guo, S., Xu, Y., Liu, H., Mao, Z., Zhang, C., Ma, Y., Zhang, Q. *et al.* (2013) The interaction between *OsMADS57* and *OsTB1* modulates rice tillering via *DWARF14*. *Nat. Commun.* **4**, 1566.
- Guo, H., Zeng, Y., Li, J., Ma, X., Zhang, Z., Lou, Q., Li, J. *et al.* (2020) Differentiation, evolution and utilization of natural alleles for cold adaptability at the reproductive stage in rice. *Plant Biotechnol. J.* **18**, 2491–2503.
- Hogan, D.J., Riordan, D.P., Gerber, A.P., Herschlag, D. and Brown, P.O. (2008) Diverse RNA-binding proteins interact with functionally related sets of RNAs, suggesting an extensive regulatory system. *PLoS Biol.* **6**, 2297–2313.
- Huang, X., Wei, X., Sang, T., Zhao, Q., Feng, Q., Zhao, Y., Li, C. *et al.* (2010) Genome-wide association studies of 14 agronomic traits in rice landraces. *Nat. Genet.* **42**, 961–976.
- Huang, X., Kurata, N., Wei, X., Wang, Z.-X., Wang, A., Zhao, Q., Zhao, Y. *et al.* (2012) A map of rice genome variation reveals the origin of cultivated rice. *Nature* **490**, 497–501.
- Huang, X., Yang, S., Gong, J., Zhao, Q., Feng, Q., Zhan, Q., Zhao, Y. *et al.* (2016) Genomic architecture of heterosis for yield traits in rice. *Nature* **537**, 629–633.
- Ishikawa, S., Maekawa, M., Arite, T., Onishi, K., Takamura, I. and Kyoizuka, J. (2005) Suppression of tiller bud activity in tillering dwarf mutants of rice. *Plant Cell Physiol.* **46**, 79–86.

- Jiang, L., Liu, X., Xiong, G., Liu, H., Chen, F., Wang, L., Meng, X. et al. (2013) DWARF 53 acts as a repressor of strigolactone signalling in rice. *Nature* **504**, 401–405.
- Jiao, Y., Wang, Y., Xue, D., Wang, J., Yan, M., Liu, G., Dong, G. et al. (2010) Regulation of *OsSPL14* by *OsmiR156* defines ideal plant architecture in rice. *Nat. Genet.* **42**, 541–544.
- Kenan, D.J., Query, C.C. and Keene, J.D. (1991) RNA recognition: towards identifying determinants of specificity. *Trends Biochem. Sci.* **16**, 214–220.
- Khush, G.S. (1995) Breaking the yield frontier of rice. *GeoJournal* **35**, 329–332.
- Kuo, A.J., Song, J., Cheung, P., Ishibe-Murakami, S., Yamazoe, S., Chen, J.K., Patel, D.J. et al. (2012) The BAH domain of ORC1 links H4K20me2 to DNA replication licensing and Meier-Gorlin syndrome. *Nature* **484**, 115–119.
- Li, X., Qian, Q., Fu, Z., Wang, Y., Xiong, G., Zeng, D., Wang, X. et al. (2003) Control of tillering in rice. *Nature* **422**, 618–621.
- Li, S., Yang, Z., Du, X., Liu, R., Wilkinson, A.W., Gozani, O., Jacobsen, S.E. et al. (2016) Structural basis for the unique multivalent readout of unmodified H3 tail by *Arabidopsis* ORC1b BAH-PHD cassette. *Structure* **24**, 486–494.
- Li, Z., Fu, X., Wang, Y., Liu, R. and He, Y. (2018) Polycomb-mediated gene silencing by the BAH-EMF1 complex in plants. *Nat. Genet.* **50**, 1254–1261.
- Li, J., Zeng, Y., Pan, Y., Zhou, L., Zhang, Z., Guo, H., Lou, Q. et al. (2021) Stepwise selection of natural variations at *CTB2* and *CTB4a* improves cold adaptation during domestication of *japonica* rice. *New Phytol.* **231**, 1056–1072.
- Liu, D. and Cai, X. (2013) *OsRRMh*, a *Spen*-like gene, plays an important role during the vegetative to reproductive transition in rice. *J. Integr. Plant Biol.* **55**, 876–887.
- Liu, W., Wu, C., Fu, Y., Hu, G., Si, H., Zhu, L., Luan, W. et al. (2009) Identification and characterization of *HTD2*: a novel gene negatively regulating tiller bud outgrowth in rice. *Planta* **230**, 649–658.
- Liu, Y., Wang, H., Jiang, Z., Wang, W., Xu, R., Wang, Q., Zhang, Z. et al. (2021) Genomic basis of geographical adaptation to soil nitrogen in rice. *Nature* **590**, 600–605.
- Livak, K.J. and Schmittgen, T.D. (2001) Analysis of relative gene expression data using real-time quantitative PCR and the $2^{-\Delta\Delta CT}$ method. *Methods* **25**, 402–408.
- Lu, Z., Yu, H., Xiong, G., Wang, J., Jiao, Y., Liu, G., Jing, Y. et al. (2013) Genome-wide binding analysis of the transcription activator IDEAL PLANT ARCHITECTURE1 reveals a complex network regulating rice plant architecture. *Plant Cell* **25**, 3743–3759.
- Lu, Z., Shao, G., Xiong, J., Jiao, Y., Wang, J., Liu, G., Meng, X. et al. (2015a) *MONOCULM 3*, an ortholog of *WUSCHEL* in rice, is required for tiller bud formation. *J. Genet. Genomics* **42**, 71–78.
- Lu, G., Coneva, V., Casaretto, J.A., Ying, S., Mahmood, K., Liu, F., Nambara, E. et al. (2015b) *OSPNSb* modulates rice (*Oryza sativa*) plant architecture and yield by changing auxin homeostasis, transport and distribution. *Plant J.* **83**, 913–925.
- Lv, Q., Li, W., Sun, Z., Ouyang, N., Jing, X., He, Q., Wu, J. et al. (2020) Resequencing of 1,143 *indica* rice accessions reveals important genetic variations and different heterosis patterns. *Nat. Commun.* **11**, 4778.
- Ma, X., Li, F., Zhang, Q., Wang, X., Guo, H., Xie, J., Zhu, X. et al. (2020) Genetic architecture to cause dynamic change in tiller and panicle numbers revealed by genome-wide association study and transcriptome profile in rice. *Plant J.* **104**, 1603–1616.
- Minakuchi, K., Kameoka, H., Yasuno, N., Umehara, M., Luo, L., Kobayashi, K., Hanada, A. et al. (2010) FINE CULM1 (FC1) works downstream of strigolactones to inhibit the outgrowth of axillary buds in rice. *Plant Cell Physiol.* **51**, 1127–1135.
- Miura, K., Ikeda, M., Matsubara, A., Song, X.-J., Ito, M., Asano, K., Matsuoka, M. et al. (2010) *OsSPL14* promotes panicle branching and higher grain productivity in rice. *Nat. Genet.* **42**, 545–549.
- Miyazaki, S., Sato, Y., Asano, T., Nagamura, Y. and Nonomura, K.I. (2015) Rice MEL2, the RNA recognition motif (RRM) protein, binds in vitro to meiosis-expressed genes containing U-rich RNA consensus sequences in the 3'-UTR. *Plant Mol. Biol.* **89**, 293–307.
- Mjomba, F.M., Zheng, Y., Liu, H., Tang, W., Hong, Z., Wang, F. and Wu, W. (2016) Homeobox is pivotal for *OsWUS* controlling tiller development and female fertility in rice. *G3-Genes Genomes Genet.* **6**, 2013–2021.
- Nonomura, K.I., Eiguchi, M., Nakano, M., Takashima, K., Komeda, N., Fukuchi, S., Miyazaki, S. et al. (2011) A novel RNA-recognition-motif protein is required for premeiotic G1/S-phase transition in rice (*Oryza sativa* L.). *PLoS Genet.* **7**, e1001265.
- Oikawa, T. and Kyozuka, J. (2009) Two-step regulation of *LAX PANICLE1* protein accumulation in axillary meristem formation in rice. *Plant Cell* **21**, 1095–1108.
- Pineiro, M., Gomez-Mena, C., Schaffer, R., Martinez-Zapater, J.M. and Coupland, G. (2003) Early bolting in short days is related to chromatin remodeling factors and regulates flowering in *Arabidopsis* by repressing *FT*. *Plant Cell* **15**, 1552–1562.
- Roundtree, I.A., Evans, M.E., Pan, T. and He, C. (2017) Dynamic RNA modifications in gene expression regulation. *Cell* **169**, 1187–1200.
- Sato, Y., Antonio, B.A., Namiki, N., Takehisa, H., Minami, H., Kamatsuki, K., Sugimoto, K. et al. (2011) RiceXPro: a platform for monitoring gene expression in *japonica* rice grown under natural field conditions. *Nucleic Acids Res.* **39**, D1141–D1148.
- Saze, H., Kitayama, J., Takashima, K., Miura, S., Harukawa, Y., Ito, T. and Kakutani, T. (2013) Mechanism for full-length RNA processing of *Arabidopsis* genes containing intragenic heterochromatin. *Nat. Commun.* **4**, 2301.
- Song, X., Lu, Z., Yu, H., Shao, G., Xiong, J., Meng, X., Jing, Y. et al. (2017) IPA1 functions as a downstream transcription factor repressed by D53 in strigolactone signaling in rice. *Cell Res.* **27**, 1128–1141.
- Sun, H., Qian, Q., Wu, K., Luo, J., Wang, S., Zhang, C., Ma, Y. et al. (2014) Heterotrimeric G proteins regulate nitrogen-use efficiency in rice. *Nat. Genet.* **46**, 652–656.
- Tabuchi, H., Zhang, Y., Hattori, S., Omae, M., Shimizu-Sato, S., Oikawa, T., Qian, Q. et al. (2011) *LAX PANICLE2* of rice encodes a novel nuclear protein and regulates the formation of axillary meristems. *Plant Cell* **23**, 3276–3287.
- Takeda, T., Suwa, Y., Suzuki, M., Kitano, H., Ueguchi-Tanaka, M., Ashikari, M., Matsuoka, M. et al. (2003) The *OSTB1* gene negatively regulates lateral branching in rice. *Plant J.* **33**, 513–520.
- Tanaka, W., Ohmori, Y., Ushijima, T., Matsusaka, H., Matsushita, T., Kumamaru, T., Kawano, S. et al. (2015) Axillary meristem formation in rice requires the *WUSCHEL* ortholog *TILLERS ABSENT1*. *Plant Cell* **27**, 1173–1184.
- Tong, H., Jin, Y., Liu, W., Li, F., Fang, J., Yin, Y., Qian, Q. et al. (2009) DWARF AND LOW-TILLERING, a new member of the GRAS family, plays positive roles in brassinosteroid signaling in rice. *Plant J.* **58**, 803–816.
- Virk, P.S., Khush, G.S. and Peng, S. (2004) Breeding to enhance yield potential of rice at IRR: the ideotype approach. *Int. Rice Res. Notes.* **29**, S1–S9.
- Wang, Y. and Li, J. (2006) Genes controlling plant architecture. *Curr. Opin. Biotechnol.* **17**, 123–129.
- Wang, X., Duan, C.-G., Tang, K., Wang, B., Zhang, H., Lei, M., Lu, K. et al. (2013) RNA-binding protein regulates plant DNA methylation by controlling mRNA processing at the intronic heterochromatin-containing gene *IBM1*. *Proc. Natl. Acad. Sci. U. S. A.* **110**, 15467–15472.
- Wang, C., Shen, L., Fu, Y., Yan, C. and Wang, K. (2015) A simple CRISPR/Cas9 system for multiplex genome editing in rice. *J. Genet. Genomics* **42**, 703–706.
- Wang, S., Wu, K., Qian, Q., Liu, Q., Li, Q., Pan, Y., Ye, Y. et al. (2017) Non-canonical regulation of SPL transcription factors by a human OTUB1-like deubiquitinase defines a new plant type rice associated with higher grain yield. *Cell Res.* **27**, 1142–1156.
- Wang, W., Mauleon, R., Hu, Z., Chebotarov, D., Tai, S., Wu, Z., Li, M. et al. (2018) Genomic variation in 3,010 diverse accessions of Asian cultivated rice. *Nature* **557**, 43–49.
- Wang, F., Han, T., Song, Q., Ye, W., Song, X., Chu, J., Li, J. et al. (2020) The rice circadian clock regulates tiller growth and panicle development through strigolactone signaling and sugar sensing. *Plant Cell* **32**, 3124–3138.
- Wu, K., Wang, S., Song, W., Zhang, J., Wang, Y., Liu, Q., Yu, J. et al. (2020) Enhanced sustainable green revolution yield via nitrogen-responsive chromatin modulation in rice. *Science* **367**, eaaz2046.
- Xie, W., Wang, G., Yuan, M., Yao, W., Lyu, K., Zhao, H., Yang, M. et al. (2015) Breeding signatures of rice improvement revealed by a genomic variation map from a large germplasm collection. *Proc. Natl. Acad. Sci. U. S. A.* **112**, E5411–E5419.

- Xing, H.-L., Dong, L., Wang, Z.-P., Zhang, H.-Y., Han, C.-Y., Liu, B., Wang, X.-C. *et al.* (2014) A CRISPR/Cas9 toolkit for multiplex genome editing in plants. *BMC Plant Biol.* **14**, 327–338.
- Yang, Z., Qian, S., Scheid, R.N., Lu, L., Chen, X., Liu, R., Du, X. *et al.* (2018) EBS is a bivalent histone reader that regulates floral phase transition in *Arabidopsis*. *Nat. Genet.* **50**, 1247–1253.
- You, L., Lin, J., Xu, H., Chen, C., Chen, J., Zhang, J., Zhang, J. *et al.* (2021) Intragenic heterochromatin-mediated alternative polyadenylation modulates miRNA and pollen development in rice. *New Phytol.* **232**, 835–852.
- Yu, S., Xu, W., Vijayakumar, C.H., Ali, J., Fu, B., Xu, J., Jiang, Y. *et al.* (2003) Molecular diversity and multilocus organization of the parental lines used in the International Rice Molecular Breeding Program. *Theor. Appl. Genet.* **108**, 131–140.
- Zhang, Z., Li, J., Yao, G., Zhang, H., Dou, H., Shi, H. and Sun, X. (2011a) Fine mapping and cloning of the grain number per-panicle gene (*Gnp4*) on chromosome 4 in rice (*Oryza sativa* L.). *Agric. Sci. China* **10**, 1825–1833.
- Zhang, H., Zhang, D., Wang, M., Sun, J., Qi, Y., Li, J., Wei, X. *et al.* (2011b) A core collection and mini core collection of *Oryza sativa* L. in China. *Theor. Appl. Genet.* **122**, 49–61.
- Zhang, H., Gao, S., Lercher, M.J., Hu, S. and Chen, W.-H. (2012) EvoView, an online tool for visualizing, annotating and managing phylogenetic trees. *Nucleic Acids Res.* **40**, W569–W572.
- Zhang, Z., Li, J., Pan, Y., Li, J., Zhou, L., Shi, H., Zeng, Y. *et al.* (2017) Natural variation in *CTB4a* enhances rice adaptation to cold habitats. *Nat. Commun.* **8**, 14788.
- Zhang, Z., Li, J., Tang, Z., Sun, X., Zhang, H., Yu, J., Yao, G. *et al.* (2018) *Gnp4/LAX2*, a RAWUL protein, interferes with the OsIAA3-OsARF25 interaction to regulate grain length via the auxin signaling pathway in rice. *J. Exp. Bot.* **69**, 4723–4737.
- Zhang, Y.-Z., Yuan, J., Zhang, L., Chen, C., Wang, Y., Zhang, G., Peng, L. *et al.* (2020) Coupling of H3K27me3 recognition with transcriptional repression through the BAH-PHD-CPL2 complex in *Arabidopsis*. *Nat. Commun.* **11**, 6212.
- Zhao, J., Wang, T., Wang, M., Liu, Y., Yuan, S., Gao, Y., Yin, L. *et al.* (2014) DWARF3 participates in an SCF complex and associates with DWARF14 to suppress rice shoot branching. *Plant Cell Physiol.* **55**, 1096–1109.
- Zhao, T., Ren, L., Zhao, Y., You, H., Zhou, Y., Tang, D., Du, G. *et al.* (2021) Reproductive cells and peripheral parietal cells collaboratively participate in meiotic fate acquisition in rice anthers. *Plant J.* **108**, 661–671.
- Zhou, F., Lin, Q., Zhu, L., Ren, Y., Zhou, K., Shabek, N., Wu, F. *et al.* (2013) D14-SCF^{D3}-dependent degradation of D53 regulates strigolactone signalling. *Nature* **504**, 406–410.

Supporting information

Additional supporting information may be found online in the Supporting Information section at the end of the article.

Dataset S1 List of the 295 varieties used in this study.

Dataset S2 The QTLs associated with tiller numbers.

Dataset S3 The candidate gene in *qTN2*.

Dataset S4 The differentially expressed genes between NIP and *tn1-1*.

Dataset S5 The alternative 3' splicing between NIP and *tn1-1* lines.

Dataset S6 Primers used in this study.

Figure S1 Population structure of 295 rice accessions.

Figure S2 Functional variation analysis of *TN1*.

Figure S3 Haplotype and expression analysis of candidate gene in *qTN2*.

Figure S4 Target sites in *tn1-2*, *tn1-3*, and *tn1-4* lines and the phenotype of *tn1-4*.

Figure S5 Comparison of tiller buds among the NIP, *tn1-1*, and *TN1-OE* lines.

Figure S6 Subcellular localization of *TN1*-GFP fusion protein in tobacco leaves.

Figure S7 Expression pattern of *TN1* in different tissues of NIP, as determined by qRT-PCR.

Figure S8 Phylogenetic analysis of TIF1 and OsEDM2 proteins and relationship of TN1 and TIF1 in tobacco leaves.

Figure S9 Interaction among TN1, TIF1, and OsEDM2.

Figure S10 Enrichment analysis of 5778 DEGs.

Figure S11 Expression levels of *DLT*, *OsTB1*, *OsPIN2*, *OsPIN5b*, and *TIF1* in NIP, *tn1-1*, and *TN1-OE* lines and expression level of *TN1* in *tif1* lines.

Figure S12 Evolutionary pattern of *TN1* based on minimum spanning.

Figure S13 Genome constitution of NIL-*TN1*^{CH1230}.

Figure S14 Haplotype analysis of *TIF1*.

Figure S15 Expression levels of *D14* among different combination of *TN1* and *TIF1* haplotypes in natural germplasm.

Figure S16 *TN1* is induced by nitrogen treatment.

Table S1 Nucleotide diversity and selection analysis of *TN1*.